Boundary-Layer Meteorol (2007) 123:295–316
DOI 10.1007/s10546-006-9143-8

ORIGINAL ARTICLE

Determining carbon isotope signatures from micrometeorological measurements: Implications for studying biosphere–atmosphere exchange processes

T. J. Griffis · J. Zhang · J. M. Baker · N. Kljun · K. Billmark

Received: 9 June 2006 / Accepted: 4 November 2006 / Published online: 23 December 2006

Abstract In recent years considerable effort has been focused on combining micrometeorological and stable isotope techniques to partition net fluxes and to study biosphere–atmosphere exchange processes. While much progress has been achieved over the last decade, some new issues are beginning to emerge as technological advances, such as laser spectroscopy, permit isotopic fluxes to be measured more easily and continuously in the field. Traditional investigations have quantified the isotopic composition of biosphere-atmosphere exchange by using the Keeling two-member mixing model (the classic Keeling plot). An alternative method, based on a new capacity to measure isotopic mixing ratios, is to determine the isotope composition of biosphere–atmosphere exchange from the ratio of flux measurements. The objective of this study was to critically evaluate these methods for quantifying the isotopic composition of ecosystem respiration (δ_R) over a period of three growing seasons (2003–2005) within a heterogeneous landscape consisting of C_3 and C_4 species. For C_4 canopies, the mixing model approach produced δ_R values that were 4–6‰ lower (isotopically lighter) than the flux-gradient method. The analyses presented here strongly suggest that differences between flux and concentration footprint functions are the main factor influencing the inequality between the mixing model and flux-gradient approaches. A mixing model approach, which is based on the concentration footprint, can have a source area influence more than 20-fold greater than the flux footprint. These results highlight the fact that isotopic flux partitioning is susceptible to problems arising from combining signals (concentration and fluxes) that

T. J. Griffis (✉) · J. Zhang · J. M. Baker · K. Billmark
Department of Soil, Water, and Climate, University of Minnesota-Twin Cities, Borlaug Hall, 1991 Upper Buford Circle, St. Paul, MN 55108, USA
e-mail: tgriffis@umn.edu

J. M. Baker
United States Department of Agriculture – Agriculture, Research Service, St. Paul, MN 55108, USA

N. Kljun
Institute for Atmospheric and Climate Science, ETH Zurich, Zurich, Switzerland

represent very different spatial scales (footprint). This problem is likely to be most pronounced within heterogeneous terrain. However, even under ideal conditions, the mismatch between concentration and flux footprints could have a detrimental impact on isotopic flux partitioning where very small differences in isotopic signals must be resolved.

Keywords Carbon cycling · Ecosystem respiration · Flux-gradient · Heterogeneous terrain · Keeling plot · Lagrangian flux and concentration footprints · Similarity theory · Stable isotopes

1 Introduction

Isotopic signatures of ecosystem–atmosphere CO_2 fluxes such as respiration (δ_R) are used to infer regional carbon sinks and sources from inversion modelling (Fung et al. 1997; Lai et al. 2004) and to partition net ecosystem CO_2 exchange (F_N) into photosynthesis (F_P) and respiration (F_R) (Yakir and Wang 1996; Bowling et al. 2001; Ogée et al. 2003; Zhang et al. 2006). δ_R represents an integrated signal, incorporating the long-term decomposition of soil organic matter, faster transformations involving autotrophic respiration, and the most rapid decomposition of labile organic carbon products. Although δ_R has been assumed to vary little temporally in land-surface and inversion models (Tans et al. 1993), recent evidence indicates substantial variation on diurnal/daily (Bowling et al. 2003; Knohl et al. 2005; Zhang et al. 2006) and seasonal time scales (Ometto et al. 2002; Griffis et al. 2005a). Uncertainty in δ_R can significantly affect ecosystem-scale flux partitioning and carbon sink/source estimates based on inverse approaches. For example, an error of 0.2‰ in the isotopic composition of soil respiration can result in an uncertainty in the terrestrial carbon sink of approximately 0.6×10^{15} g C year^{-1} (Ciais et al. 1999). There is a need, therefore, to improve our ability to quantify ecosystem-scale δ_R in order to better constrain gross flux estimates and to help resolve regional sinks/sources with greater certainty.

To date, many studies have quantified δ_R using the traditional Keeling plot (linear mixing model) method (Keeling 1958). Since the time of Keeling's classic 1958 paper, numerous investigators have extended the application of the Keeling plot to examine the isotopic signatures of both CO_2 and water vapour exchange at spatial scales ranging from small chambers up to ecosystems, and even to an extensive region (Randerson et al. 2002; Flanagan et al. 1999; Yepez et al. 2003). There are a number of methodological limitations associated with the Keeling method that have been well documented (Pataki et al. 2003). Some of these include increased uncertainty of the intercept as the concentration range decreases; uncertainty related to the extrapolation of the linear regression to the y-intercept (Yakir and Sternberg 2000); and uncertainty in the specification of the background CO_2 concentration and its isotopic ratio (Lloyd et al. 1996). No study, however, has considered problems related to flux and concentration footprints (i.e. the relative contribution of the upwind source area to the measurement), synoptic air mass trajectory, and their potential influence on the footprint function of the Keeling plot. This latter problem raises a very important question for ecosystem-scale applications—*what is the footprint function of a Keeling plot*?

As micrometeorological and isotopic techniques are increasingly being combined to study biosphere exchange processes, it is important to ensure that the isotopic

signatures and flux densities are representative of similar spatial and temporal scales and, therefore, the underlying biophysical processes. For instance, at the ecosystem scale, concentration and isotope ratio data have been combined with flux measurements to partition F_N into its primary components (Bowling et al. 2001; Lai et al. 2003; Ogée et al. 2003). It is well known, however, that the footprint function of a concentration scalar is considerably larger than that of a flux measurement made at the same point above the surface (Kljun et al. 2002; Schmid 1994, 2002). These differences result from the fact that flux footprints are sensitive to the vertical motion of the tracer. For distances close to the sensor, most of the air parcels carrying a tracer contribute positively to the flux. Tracers emitted further away from the sensor have a higher probability of travelling downwards by the time they reach the sensor, thereby, contributing negatively to the flux. Vertical motions, therefore, tend to cancel each other as the distance from the sensor increases. In contrast, the concentration footprint is sensitive to the number of tracers passing the sensor and their contributions simply add up independently of their vertical motion. The differences in footprint function can be substantial depending on atmospheric stability, surface roughness, measurement height, wind speed etc. Furthermore, the Keeling plot, which is dependent on concentration data collected over relatively long time periods (a few hours or more), may be influenced by synoptic air mass trajectory (Lee et al. 2006). Such issues bring into question the previous interpretation and inference of the isotopic composition of ecosystem respiration (δ_R), net ecosystem CO_2 exchange (δ_N) and subsequent isotopic flux partitioning at the ecosystem scale.

In this study we examine differences in the isotopic composition of ecosystem respiration (δ_R) within a landscape consisting of heterogeneous terrain, using a flux-gradient (*flux ratio*) methodology and the traditional Keeling plot technique from high-temporal resolution isotope measurements taken over a period of three growing seasons (2003–2005). The objectives are

1. Quantify the seasonal and interannual variation in the isotopic composition of ecosystem respiration (δ_R) using the traditional Keeling plot and the flux ratio methods.
2. Define and examine the footprint function of δ_R obtained using the Keeling plot and flux-gradient methods.
3. Investigate the potential influence of the two-dimensional flux footprint and air mass (back) trajectory on δ_R.

2 Methods

2.1 Study site

The research site is located near St. Paul, Minnesota (44°42′51.5″ latitude, 93°05′23.4″ longitude and 259 m.a.s.l.). The landscape can be considered highly heterogeneous with mixed agriculture (mostly pasture and row crops), remnant forest, and encroaching urban development from the north and west (Fig. 1). The field site is homogeneous and flat with an extensive fetch—more than 200 m in all directions from the micrometeorological tower. Intensive management of the site can be tracked over the last 125 years. Pre-settlement vegetation history of the region is upland dry prairie

Fig. 1 Air photo of the research study site and surrounding heterogeneous landscape. The field site is outlined using a thick dashed white line with the solid circle designating the position of the micrometeorological tower. The tower is located approximately 200 m from the edge of the field. Flux (short-dashed ellipse) and concentration (long-dashed ellipse) footprints are shown for a typical case (Table 1, September 14, 2005). The air photo is 1-m resolution, natural color imagery derived from the original uncompressed TIFF quarter-quad orthophoto, Farm Services Administration (FSA) 2003–2004 DOQs, Minnesota Department of Natural Resources

consisting of C_3 and C_4 plant species (Marschner 1974). Wheat (C_3 photosynthetic pathway) was planted as early as 1879 according to the Minnesota State Agricultural Census Data, Dakota County Historical Society. In recent years (1998–2001) the field was planted in continuous corn (*Zea mays* L., C_4 photosynthetic pathway). Detailed analyses of the carbon isotope composition of soil organic matter has shown that the upper 0.45 m of the soil organic profile is well-mixed from tillage and has a mean carbon isotopic ratio of −18‰ that varies little on a seasonal basis (Griffis et al. 2005a). Photosynthetic discrimination results in bulk isotopic signatures of −12 and −26‰ for corn (C_4) and soybean (C_3), respectively. We expect, therefore, that the C_4 canopy will act to enrich ecosystem respiration whereas the C_3 canopy will tend to deplete ecosystem respiration, depending on the relative partitioning of ecosystem respiration into its autotrophic and heterotrophic components.

The data presented here were collected during the growing seasons (≈DOY 130 to DOY 280) from 2003 to 2005 with *Zea mays* (corn, C_4 photosynthetic pathway) planted on May 2, 2003 (DOY 122), May 3, 2005 (DOY 123) and *Glycine max* (soybean, C_3 photosynthetic pathway) on May 27, 2004 (DOY 148). The respective harvest dates were October 16, 2003 (DOY 289), October 26, 2005 (DOY 299) and October 12, 2004 (DOY 286). A significant period of missing data occurred from DOY 130 to DOY 170 in 2004 due to an unfortunate cryocooler failure on the isotope tunable diode laser (TDL) system.

From a micrometeorological perspective, the site is ideal for investigating flux-gradient and concentration/flux footprint relationships because the immediate site is homogeneous, yet surrounded by a complex heterogeneous landscape. Consequently, the sensitivity of key isotopic parameters can be evaluated with respect to differences between concentration and flux footprints. A detailed description of the eddy-covariance and TDL measurement systems, flux calculations, isotope error propagation, and data handling procedures can be found in Baker and Griffis (2005) and Griffis et al. (2005a).

2.2 Keeling mixing model and isotopic fluxes

Briefly, the Keeling intercept can be derived from the following mixing relationship assuming conservation of mass,

$$c_a = c_b + c_s \tag{1a}$$

where c_a, c_b and c_s are CO_2 mixing ratios defined as total, background, and source air (ecosystem respiration), respectively. Similarly, the mass balance for $^{13}CO_2$ is given by

$$\delta_a c_a = \delta_b c_b + \delta_s c_s, \tag{1b}$$

with the products of the respective delta terms yielding approximations for the $^{13}CO_2$ mixing ratio of each component.

Combining 1a and 1b yields the isotopic composition of the source air (where $\delta_s = \delta_R$ at night, assuming photosynthetic activity is negligible),

$$\delta_a = \frac{c_b(\delta_b - \delta_s)}{c_a} + \delta_s. \tag{1c}$$

Early application of the Keeling plot relied on traditional least squares regression (Keeling 1958), but later work recommended a type II geometric regression to account for errors present in both the dependent (y) and independent (x) variables (Pataki et al. 2003 and the references therein). Recent high temporal resolution $\delta^{13}CO_2$ observations by Bowling et al. (2005) revealed anomalous Keeling intercepts for small ranges in CO_2 mixing ratio. Zobitz et al. (2006) investigated this problem further and demonstrated that the Keeling δ_R value is biased at the low CO_2 range due to the type II geometric mean regression. Based on their high resolution data and analytical review of the regression methods, they recommended the use of type I regression because the relative error in the $\delta^{13}CO_2$ measurements is significantly greater than the relative error in CO_2 mixing ratio measurements. In this study, we have computed Keeling plots following the above recommendation.

From Monin–Obukhov similarity theory (MO theory), δ_R can be obtained from the flux-gradient (*flux ratio*) relationship (Griffis et al. 2004),

$$F_N^{13} = -K_C \frac{\overline{\rho_a}}{M_a} \frac{d\overline{^{13}CO_2}}{dz} + \frac{\overline{\rho_a}}{M_a} \frac{d}{dt} \int_0^z {}^{13}CO_2(z)\, dz, \tag{2a}$$

$$F_N^{12} = -K_C \frac{\overline{\rho_a}}{M_a} \frac{d\overline{^{12}CO_2}}{dz} + \frac{\overline{\rho_a}}{M_a} \frac{d}{dt} \int_0^z {}^{12}CO_2(z)\, dz, \tag{2b}$$

where F_N^{13} and F_N^{12} are the $^{13}CO_2$ and $^{12}CO_2$ net fluxes, K_C is the eddy diffusivity of CO_2, $\overline{\rho_a}$ is the average density of dry air, M_a is the molecular weight of dry air, and $d\overline{^{13}CO_2}/dz$, $d\overline{^{12}CO_2}/dz$ are the time-averaged mixing ratio gradients of $^{13}CO_2$ and $^{12}CO_2$ measured simultaneously at the same heights using TDL spectroscopy (TGA100, Campbell Scientific Inc., Logan, UT). The second term on the right-hand side of Eqs. 2a and 2b represents the rate of change of storage for each of the isotopologues. These terms are negligible when the friction velocity (u_*) is greater than $0.1\ m\ s^{-1}$. In the flux ratio approach, similarity in the eddy diffusivity is assumed for $^{12}CO_2$ and $^{13}CO_2$, reducing the problem to a measurement of the $d^{13}CO_2/d^{12}CO_2$ gradient or finite difference. The isotopic composition of ecosystem respiration, obtained from nighttime flux ratios, is expressed in delta notation (a dimensionless factor of parts per thousand, ‰) relative to the Vienna Peedee Belemnite scale (R_{VPDB}),

$$\delta_R = 1000\left(\frac{\overline{d^{13}CO_2}/\overline{d^{12}CO_2}}{R_{VPDB}} - 1\right). \quad (3)$$

2.3 Tunable diode laser sampling scheme

The TDL system used in this study has been described previously by Griffis et al. (2004, 2005b). The half-hourly measurement precisions for $^{12}CO_2$, $^{13}CO_2$, and $\delta^{13}C$ are $\pm 0.03\,\mu mol\,mol^{-1}$, $0.0002\,\mu mol\,mol^{-1}$ and 0.07‰, respectively. The sampling strategy varied over the duration of this experiment. In 2003 (C_4, corn canopy), four sample inlets were used and their heights were adjusted according to canopy development. The TDL computer controlled the sampling system with parameters set to cycle through the four sample inlets and two calibration standards within a 2-min sample period ($T_c = 120\,s$). This sequence included calibration using $\approx 350\,\mu mol\,mol^{-1}$ CO_2 with known isotopic ratio; calibration using $\approx 600\,\mu mol\,mol^{-1}$ CO_2 with known isotope ratio; measurement of CO_2 mixing ratio above the canopy at a heights z_4 and z_3; measurement of CO_2 mixing ratio within the canopy at z_2 and z_1. The above-canopy sample inlets (z_3 and z_4) were positioned at heights of 2.00 and 2.35 m and raised to heights of 3.30 and 3.65 m on July 17 (DOY 198) in relation to the changing canopy height. Sample inlets within the canopy were positioned at a height of 1 m. Inlet z_2 was used for performing zero gradient tests and was frequently repositioned. Within each 2-min cycle each sample and calibration inlet was sampled for 20 s. In 2004 (C_3, soybean canopy), two sample inlets were used at fixed heights above the canopy. The upper inlet (z_2) was positioned at 2.50 m and the lower inlet (z_1) at 1.85 m. The sampling sequence was similar to above, beginning with two calibration standards and then sampling the upper and lower inlets within a 2-min cycle. In this case, the calibration standards were each sampled for 20 s and each sample inlet for 40 s. In 2005 (C_4, corn canopy), two sample inlets were used and their heights were adjusted with canopy development. Prior to June 30 (DOY 181) the lower sample inlet (z_1) was positioned at 2.00 m and the upper inlet (z_2) at 3.50 m. The inlets were raised to 3.10 and 4.20 m, respectively after DOY 181. The same sampling sequence was used in both 2004 and 2005. For reference, Fig. 2 shows the canopy height (h_c) and the relative height of the lowest inlet above the canopy during each field campaign. We note that during the mid growing period the lowest sample inlet above the corn canopy was only $1.2\,h_c$—a constraint imposed by the fetch limitation and gradient resolution.

TDL isotope analyzers offer great improvement in measurement frequency over traditional flask sampling and mass spectrometry analysis. However, since concentrations are not measured simultaneously at each inlet, care must be taken to ensure that the gradient sampling scheme adequately approximates the true variations in the profile. In 2004 and 2005 we introduced small buffer volumes (150 ml) into the sampling system to damp turbulent fluctuations and reduce the loss of profile information. Typical nighttime power spectra ($S_x(f)$) for CO_2, based on 10 Hz open-path infrared gas measurements (LI-7500, Licor Inc., Lincoln NE), taken between 2200 and 0400 h local time during the peak growing period revealed that the maximum power occurs at a corresponding frequency (f_{peak}) of 0.003 and 0.02 Hz over the corn and soybean canopy, respectively. The corresponding turbulent time scales ($\tau = 1/f_{peak}$), therefore, are on the order of 330 and 50 s. Following Meyers et al. (1996) and Woodruff (1986), the relative sampling error (ε) can be inferred from: $\varepsilon = 6\left(\frac{T_c}{\tau}\right)^{0.8}$. For the above cases, the typical error is estimated between 3 and 12%. Although the

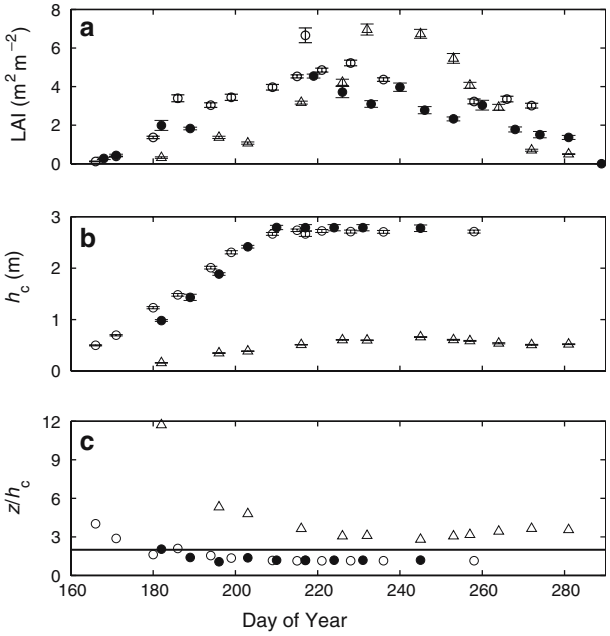

Fig. 2 Phenological development of the canopy. Closed circles, open triangles, and open circles represent corn 2003 (C_4), soybean 2004 (C_3), and corn 2005 (C_4), respectively. Leaf area index (**a**); canopy height (**b**); and the ratio of the above-canopy TDL inlet to canopy height (**c**) are shown. The solid line represents $z/h_c = 2$

sampling error is relatively small, it remains a difficult challenge to resolve small isotopic gradients. The relative error propagating into the flux calculations is approximately 25% for $^{12}CO_2$ and $^{13}CO_2$ (Griffis et al. 2004). Zhang et al. (2006) have shown that the uncertainty in the half-hourly flux ratio method, for $u_* > 0.1$ m s^{-1}, is typically ±2‰. Averaging over the nighttime period (2200–0400 h local time) reduces the uncertainty of the flux ratio to about ±0.7‰. Error estimates of the Keeling plot intercepts over the same time period are typically 0.4‰ (Griffis et al. 2005a; Zhang et al. 2006).

2.4 Footprint function calculations

Footprint estimates were derived using the three-dimensional Lagrangian stochastic model LPDM-B of Kljun et al. (2002). Unlike most other Lagrangian stochastic particle models, LPDM-B is not only valid for one given stability regime, but is designed for boundary-layer conditions ranging from stable to convective. In LPDM-B, the emitted tracer is simulated as the release of a large number of particles, which are assumed to follow the flow exactly. The particles are tracked backwards in time, from the measurement location to the source (e.g., at the surface), using 'backward' trajectories of particles as described in Flesch et al. (1995) LPDM-B has been tested against the results of other footprint models with respect to flux and concentration footprints and also compared well with results from a wind-tunnel study (Kljun et al. 2002, 2004). The current version of the footprint model has been designed for

measurements above the roughness sublayer. Due to suppressed dispersion within the roughness sublayer, the footprints presented here might be underestimated by this model (cf. Rotach 2001), however, the relative difference between concentration and flux footprints is expected to be similar. See Kljun et al. (2002) for a complete description of the model.

3 Results and discussion

3.1 Seasonal dynamics and interannual variation of δ_R

The phenological phase has been shown to have a dominant influence on F_N and its isotopic composition (Griffis et al. 2005a). Leaf area index (LAI), canopy height (h_c), and the ratio of the above-canopy TDL inlet to canopy height (z/h_c) are shown in Fig. 2 to help better interpret the influence of canopy development on isotopic CO_2 exchange. It is also important to note that eddy-covariance flux measurements of CO_2 exchange indicate that the canopy was photosynthetically active over the periods: DOY 166 to DOY 260; DOY 177 to DOY 268; and DOY 159 to DOY 276, in 2003, 2004, and 2005, respectively.

In agricultural ecosystems, rotation between C_3 and C_4 crops can lead to a very dynamic seasonal response in the carbon isotopic signature of ecosystem respiration (Rochette et al. 1999). Figure 3 illustrates the seasonal and interannual variations in δ_R estimated using the flux ratio methodology over a period of three growing seasons. It is interesting to note the remarkable similarity in the shape of the δ_R seasonal pattern during both the 2003 and 2005 C_4 growing seasons. The rapid positive increase in δ_R for both of these years results from the strong $^{13}CO_2$ enrichment of F_R caused by increased C_4 autotrophic respiration and the microbial utilization of C_4

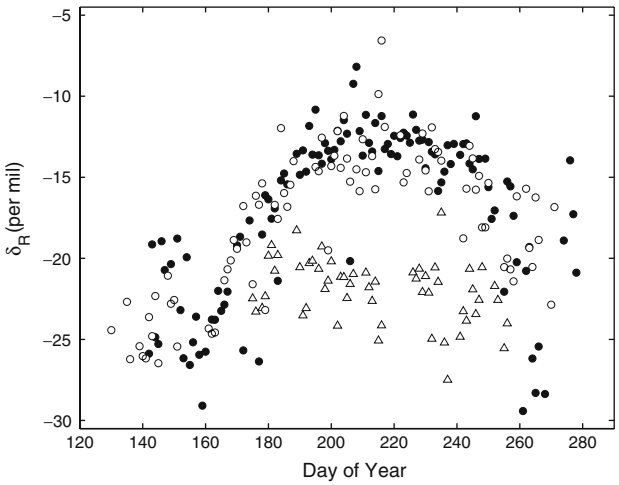

Fig. 3 Seasonal and interannual variation in the isotopic composition of ecosystem respiration measured using the flux-gradient approach. Closed circles, open triangles, and open circles represent corn 2003 (C_4), soybean 2004 (C_3), and corn 2005 (C_4), respectively. Each data point represents a single nighttime value with a time interval ranging from 2200 to 0400 local time. Standard error of the δ_R values is typically 0.7‰

root exudates. Each of the C_4 years also reveals the rapid decrease in δ_R following senescence, indicating a relative increase in heterotrophic respiration having a C_3 dominant signature.

The similarity in the seasonal progression of δ_R for each of the C_4 years shows that recent carbon fixation has a dominant influence on ecosystem respiration. It is during the transition periods (i.e. DOY 160–200) that significant differences exist between the isotopic composition of photosynthesis and ecosystem respiration—providing a best case scenario for flux partitioning (Zhang et al. 2006). During the 2004 C_3 year δ_R showed little seasonal variation because of the relatively small signal difference between autotrophic and heterotrophic respiration. A small mid-season minimum in δ_R can be observed as autotrophic respiration increased and microbial activity utilized recent root exudates. Note, however, that the values of δ_R were relatively enriched by about 4‰ when compared to the expected signal for C_3 respiration (i.e. −28‰), which is a result of many recent years of C_4 corn production at this site. Another interesting observation is the highly negative δ_R values observed during the non-growing season period, which we hypothesize to be a consequence of either stronger anthropogenic influence or a shift in microbial activity or substrate use at these lower temperatures. Considering that the upper midwestern United States is dominated by corn–soybean rotation ecosystems, one might expect that the strong trends in seasonal isotopic composition of F_R have an important influence on the atmosphere's isotopic carbon content and might provide a valuable diagnostic in resolving regional carbon balances.

3.2 Flux-gradient and keeling plot comparison

Initial comparison of the Keeling plot and flux-gradient (flux ratio) method were made following soybean harvest in autumn 2002 (Griffis et al. 2004). These early results showed relatively good agreement for non-growing season conditions (October 25–November 19, 2002) with δ_R estimates characteristic of a C_3 (soybean) signal. Small differences were observed between each method and at that time were interpreted as uncertainties related to low biological activity and small fluxes. Figure 4 illustrates the Keeling plot and flux ratio estimates of δ_R for the 2005 C_4 growing season. This particular result reveals that the two approaches agree reasonably well for the non-growing season, but that an exceptional difference (>6‰) develops as the canopy matures. This difference was also observed by Zhang et al. (2006) for the 2003 C_4 growing season. Examination of all data collected over the period 2003–2005 reveals an important pattern with the C_4 non-growing season and C_3 growing season data collapsing on the 1:1 line in Fig. 5. The growing season C_4 data, however, indicate a significant offset from the 1:1 line. Three hypotheses are proposed to explain the differences in δ_R resulting from each approach:

I. Monin–Obukhov similarity theory fails when applied to the flux-gradient (flux ratio) approach over the taller C_4 corn canopy because the near-field effect decouples the vertical gradient (dc/dz) from the local vertical flux density.
II. The two-dimensional footprint of δ_R derived from the flux ratio methodology is heavily weighted toward the top of the canopy under stable atmospheric conditions and consequently bears an isotopic signal biased toward autotrophic respiration.

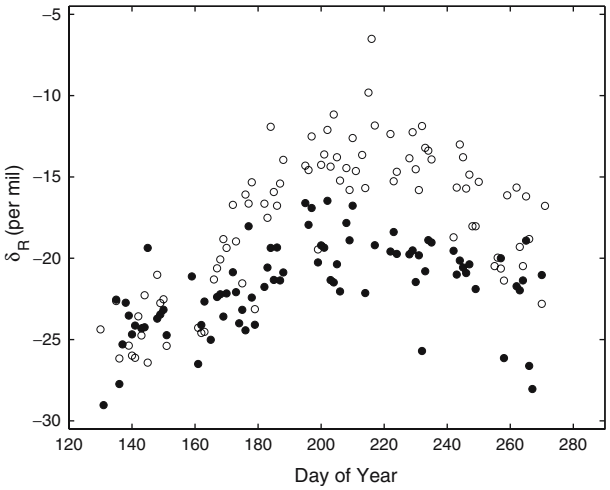

Fig. 4 Seasonal variation in the isotopic composition of ecosystem respiration quantified using the flux-gradient (open circles) and mixing model/Keeling (closed circle) approach for the 2005 corn (C_4) canopy. Each data point represents a single nighttime value with a time interval ranging from 2200 to 0400 local time. Standard error of the Keeling and flux-gradient δ_R values is typically 0.4‰ and 0.7‰, respectively

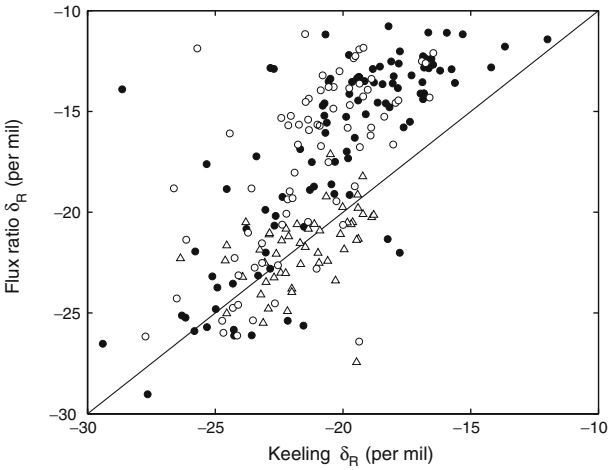

Fig. 5 Comparison of the mixing model and flux-gradient estimates of δ_R. Closed circles, open triangles, and open circles represent the isotopic composition of ecosystem respiration measured in 2003 (corn, C_4), 2004 (soybean, C_3), and 2005 (corn, C_4), respectively

III. The footprint function of a Keeling plot (concentration footprint) extends beyond the ecosystem scale of interest and is therefore not representative of the ecosystem-scale processes that are typically investigated using flux-based (gradient or eddy covariance) approaches.

3.3 Flux-gradient approach: within and above-canopy measurements

Eddy-covariance (EC) and flux-gradient (FG) measurements of total CO_2 exchange were compared to gain insight regarding the potential failure of MO theory and its relation to estimating δ_R (Hypothesis I). Figure 6 shows a comparison of EC and FG derived CO_2 fluxes for an ensemble diurnal period during the early growing season (DOY 170–183, C_4 - year 2005) when the flux ratio and Keeling methods differed by about 3‰. The canopy height and LAI ranged from 0.7 to 1.4 m and 0.30 to 1.8 $m^2\ m^{-2}$, respectively. In this case, the lower air sample inlet above the canopy was approximately $1.5h_c$. This 2-week period illustrates good agreement between the EC and FG approaches for both daytime and nighttime periods. On average, the enhancement factor (γ = EC/FG) was 1.06 ± 0.57 (± 1 standard deviation) over the entire diurnal period. γ was significantly smaller than the values reported by Simpson et al. (1998) for flux-gradient measurements made over a forest at $1.4–1.6h_c$ for atmospheric stability (z/L) ranging from -2 to 0.4, L being the Obukhov length.

For the period DOY 230 to DOY 243, the canopy had reached its maximum height (2.8 m) and LAI ($4\ m^2\ m^{-2}$), while the lowest air sample inlet was only $1.2h_c$ and presumably more strongly influenced by the near-field effect of the canopy (Kaimal and Finnigan 1994; Raupach 1989). The near-field effect would be most pronounced at night when the Lagrangian time scale for vertical velocity (τ_L) typically attains its largest value (≈6 s for this particular case). One might expect, therefore, that the gradient (dc/dz) would become decoupled from the scalar flux density (Raupach 1989). The difference between the Keeling and flux ratio estimates of δ_R was often greater

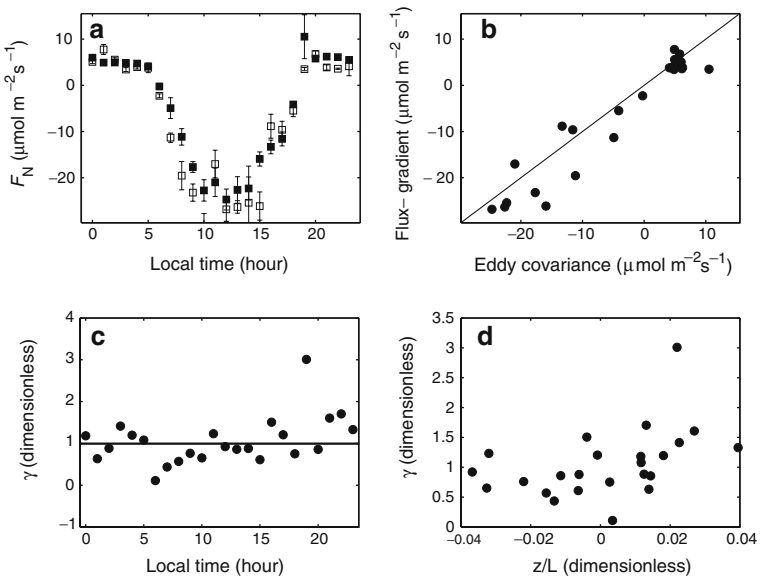

Fig. 6 Comparison of CO_2 fluxes estimated from eddy covariance (closed squares) and Monin–Obukhov similarity theory (open squares) over a developing corn canopy during the early growing period (DOY 170–183) of 2005. Diurnal comparison of fluxes (**a**), 1:1 plot (**b**), diurnal variation in enhancement factor (**c**), and dependence of enhancement factor on Obukhov length scale (**d**). Note that flux-gradient calculations were made following the method of Simpson et al. (1998)

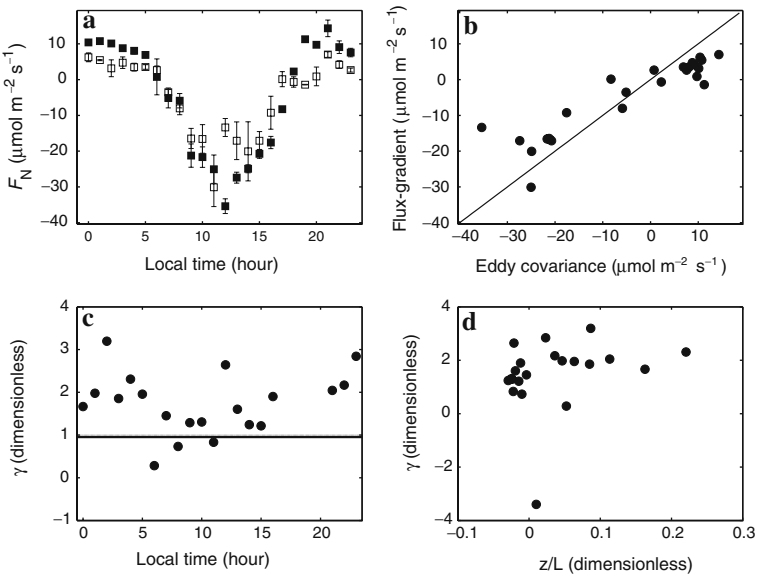

Fig. 7 Comparison of CO_2 fluxes estimated from eddy covariance (closed squares) and Monin–Obukhov similarity theory (open squares) over a developing corn canopy during the early growing period (DOY 230–243) of 2005. Diurnal comparison of fluxes (**a**), 1:1 plot (**b**), diurnal variation in enhancement factor (**c**), and dependence of enhancement factor on Obukhov length scale (**d**)

than 5‰ during this period. Figure 7 illustrates that FG exchange was substantially smaller than the EC estimate ($\gamma = 2.16 \pm 1.32$); the difference was most pronounced during stable nighttime conditions, despite using a u_* filter of 0.1 m s^{-1}. A number of studies have shown that MO theory breaks down within the roughness sublayer over taller vegetation (Denmead and Bradley 1985) leading to a large underestimate of the flux. This has been attributed to the fact that the length scale of the curvature of the concentration gradient is less than the length scale of eddies that dominate the scalar transport, resulting in unrealistic (i.e. sometimes negative) values of eddy diffusivity and countergradient scalar transport, (Corrsin 1974). Further, the large coherent eddies generated by shear instability act to enhance the eddy diffusivity near the top of the canopy (Lee 2003). Careful experiments by Simpson et al. (1998) demonstrated that above a forest FG measurements were in relatively good agreement with EC measurements at 1.9 and 2.2h_c, while measurements closer to the surface (i.e. 1.2–1.4h_c) showed larger differences, with enhancement factors ranging from 1.6 to 1.8. These enhancement factors can be reproduced reasonably well from localized near-field theory (Lee 2003). While it is clear from the large body of evidence in the literature that the FG approach underestimates the scalar transport when applied too close to the canopy, it does not appear that the breakdown of MO theory is the main factor for the observed difference in isotopic composition between the flux ratio and Keeling methods. As shown above, relatively large differences in δ_R (3‰) were observed for cases when the FG and EC methods were in very close agreement—suggesting that dc/dz was not significantly decoupled from the local vertical flux density.

Hypothesis II considers the potential influence of having strong differences in isotopic signals between the soil and vegetation. Recent work (Lee 2003, 2004)

examined the two-dimensional (streamwise and vertical) flux footprint, considering dual/elevated sources as observed by a measurement system located within the roughness sublayer. A number of key results emerged from these studies that may have important implications for the interpretation of isotopic flux measurements and flux partitioning. First, for unstable atmospheric conditions the two-dimensional flux footprint was shown to be more heavily weighted toward the lower canopy (i.e. a stronger soil signal with respect to the carbon flux). Second, for stable atmospheric conditions the flux footprint was weighted more heavily toward the upper canopy (i.e. a stronger autotrophic signal with respect to the carbon flux). Third, under stable conditions the extensive flux footprint and the mismatch between the ground and elevated sources can be substantial. Such differences in the source footprint function could potentially have broad implications for interpreting flux measurements and partitioning net fluxes into their components when using isotope signals. It is well established that MO theory cannot be applied within canopies to estimate scalar transport due to countergradient flow (Denmead and Bradley 1985; Raupach 1989). Griffis et al. (2005a), however, demonstrated that within-canopy isotopic flux ratios were not statistically different from above-canopy flux ratios during the 2003 C_4 (corn) growing season (despite observation of countergradients). For relatively short stature vegetation, therefore, the flux isotope ratio appears to be a relatively conservative property of the canopy–atmosphere exchange even for situations when the differences between the isotopic composition of the soil and elevated vegetation sources are potentially very large—at least 6‰ in this case. Figure 8 provides further support of this view by examining the isotopic ratio of the change in CO_2 storage (iso-storage, second term in Eq. 2) for the nighttime period (C_4, 2003). These results illustrate moderate correlation with the above-canopy flux ratios and more importantly do not suggest any significant bias. These data provide reasonably strong evidence that differences related to the two-dimensional nature of the flux footprint are not the main factor determining the bias in the isotopic signature of ecosystem respiration for the Keeling versus flux ratio methods.

3.4 What is the footprint function of δ_R?

Hypothesis III considers the problem of combining concentration and flux information at the ecosystem scale. Daytime and nighttime hourly histograms of σ_w, u_* and z/L are shown in Figs. 9 and 10, respectively for the period DOY 200–230 during the C_4 2005 growing season. These data were used to derive the typical footprint function of δ_R associated with the nighttime flux ratio method shown in Fig. 11. A subset of these data has shown that the nighttime median value of σ_w ($0.13\,m\,s^{-1}$) is typically associated with u_* and z/L values of $0.09\,m\,s^{-1}$ and 0.44, respectively. For typical conditions, therefore, the flux footprint extends out to about 100 m from the measurement tower (at the 90% contribution level) and is well within the fetch limits (200 m) of the tower/field. As expected, the concentration footprint for a single level above the canopy is dramatically larger, extending out to distances of 2500 m (greater than 10-fold the scale of the maximum fetch and 20-fold greater than the scale of the flux footprint). Figure 11 also shows that daytime concentration and flux footprints are considerably smaller than at night, which might raise other scaling issues related to the extrapolation of nighttime data to daytime conditions for the purpose of flux partitioning using either standard micrometeorological or isotopic techniques. An important point is that the Keeling plot works best when the concentration range is

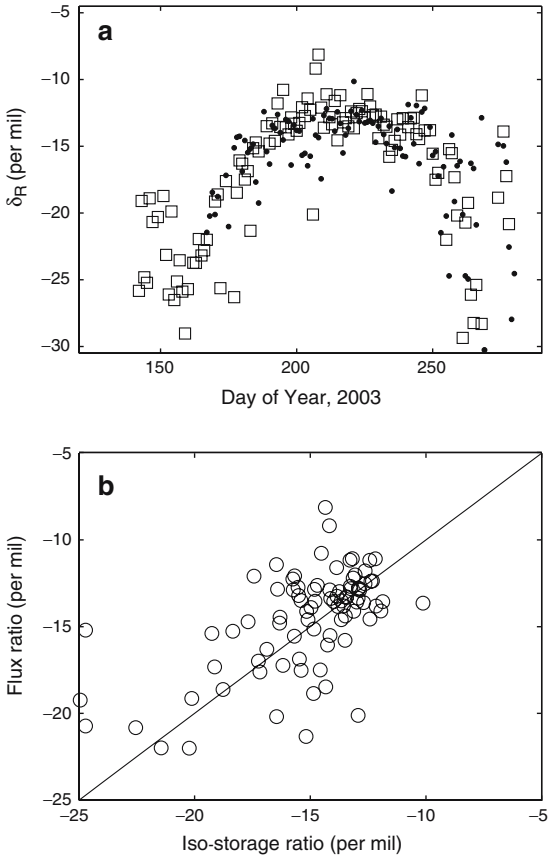

Fig. 8 Isotopic composition of canopy CO_2 storage term and above-canopy fluxes during the 2005 growing season. Seasonal variability in the isotopic composition of CO_2 storage (closed circles) and above-canopy fluxes (open squares) are shown (**a**). Comparison of the isotopic composition of the CO_2 storage term and the above-canopy fluxes is shown in the 1:1 plot (**b**)

large (Pataki et al. 2003) and these conditions coincide with the development of stable nighttime conditions when the concentration footprint is greatest.

We used a simple zero-dimensional box model (Seinfeld and Pandis 1998) to explore the potential influence of the concentration footprint on the Keeling plot estimates of δ_R. The mixing height of the box (H) was defined as the nocturnal boundary-layer depth, which is typically about 500 m, based on morning soundings from the local weather station (Channhassen, MN, Station 72649 MPX). The horizontal dimensions of the box (dx) are defined by the along-wind extent of the concentration footprint. Entrainment can be ignored for the nocturnal boundary-layer case and the concentration change with time (dc/dt) for each inert isotopologue inside the box can be approximated from,

$$\frac{dc}{dt} = \frac{F_N}{H} + \frac{(c_b - c_i)}{\tau}. \tag{4a}$$

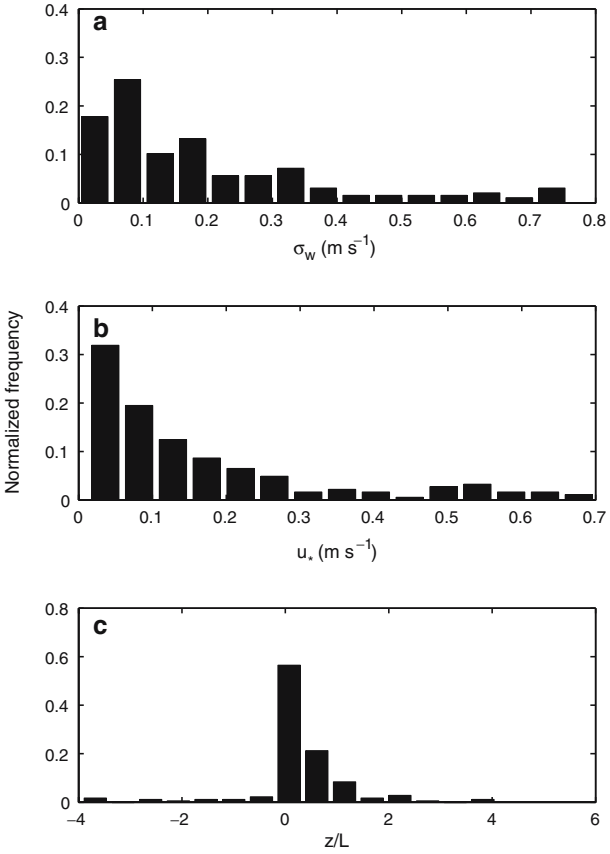

Fig. 9 Mid-growing season nighttime (2200 to 0400 local time) histograms of the standard deviation of vertical wind velocity (**a**), friction velocity (**b**), and Obukhov length (**c**)

At $t = 0, c_i = c_i(0)$ and therefore,

$$c_i(t) = c_i(0)\mathrm{e}^{-t/\tau} + \left(\frac{F_N}{H} + c_\mathrm{b}\right)\left(1 - \mathrm{e}^{-t/\tau}\right), \tag{4b}$$

where c_b is the initial background concentration, t is time in seconds, and τ is the turnover time of the box obtained from the ratio of dx to average wind speed. Equation 4 can be written explicitly for each isotopologue in order to obtain δ_R from the Keeling intercept. F_N was assumed constant over the nighttime period for the entire surface area of the box, and the isotopic ratio of the flux (δ_N) was weighted according to the concentration footprint. A source value of −12‰ was assumed for C_4 vegetation between the tower and the edge of the field ($\approx$200 m) and −28‰ for any flux originating beyond the field dimensions (>200 m). Figure 12 shows simulations of Keeling plots for five cases (i.e. five different isopleths from Fig. 11) illustrating that as the concentration footprint extends the value of δ_R becomes progressively more negative (isotopically depleted with respect to $^{13}CO_2$) because of the increased relative contribution from surrounding C_3 sources. For typical nighttime conditions, therefore, the bias between the flux ratio and Keeling methods can easily be accounted for in

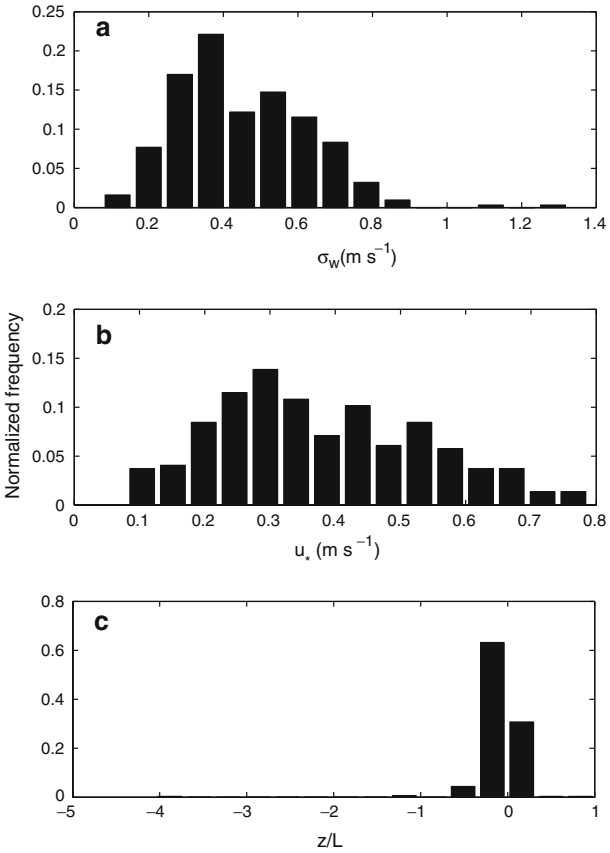

Fig. 10 Mid-growing season daytime (0600 to 1800 local time) histograms of the standard deviation of vertical wind velocity (**a**), friction velocity (**b**), and Obukhov length (**c**)

terms of footprint differences. The C_3 contamination is obviously difficult to diagnose when the source difference between the field and surroundings is small such as in the C_3-soybean case (shown in Fig. 5). However, we emphasize that in either case there is a significant contribution from sources beyond the field so that in most situations the contributions influencing the scalar concentration are likely not spatially representative of the ecosystem-scale fluxes/processes being examined unless the landscape is truly extensive and homogeneous, a condition that is rarely met.

Unfortunately, the typical footprint associated with the Keeling method is difficult to define because it is developed from observations of concentration change over relatively long time intervals (i.e. a nighttime period) where stationarity assumptions are not likely to hold. Under such conditions the change in nocturnal boundary-layer CO_2 mixing ratio is related to the net ecosystem CO_2 exchange of the underlying ecosystem, but is also influenced, to a lesser extent, by the air mass (back) trajectory. Table 1 shows typical air parcel (back) trajectories during the mid growing season of 2005 (C_4 corn year) and reveals that air masses typically originate from about 100–300 km away over a period of 6 h. Under such conditions the influence of "long distance" transport on background CO_2 mixing ratio and isotopic composition is likely to have

Table 1 The potential spatial influence on estimating δ_R

Date/DOY	δ_R-Keeling	δ_R-Flux ratio	Flux footprint[a] (m)	Concentration footprint (km)	Air mass trajectory[b] (km)
June 11, 2005 (162)	−24.1	−24.6	90	2.5	106
July 19, 2005 (200)	−19.2	−14.3	60	1.8	109
July 29, 2005 (210)	−16.8	−12.6	100	3.3	123
Aug 18, 2005 (230)	−21.5	−14.5	100	3.4	258
Sept 14, 2005 (257)	−20.6	−20.0	100	1.6	252

[a] Along-wind extent of the footprint comprising 90% of the source area, derived by Lagrangian footprint model (Kljun et al. 2004)

[b] Air mass 6-h back trajectory model analysis (NOAA-HYSPLIT) with latitudinal and longitudinal coordinates of the trajectory end points converted to angular distance

some influence on the Keeling plot parameters. In some cases we have observed air masses originating over Lake Superior that have forward trajectories coincident with our concentration measurements. The extent to which these trajectories influence the background concentration and isotopic composition is difficult to assess, and the air mass may also be heavily influenced by anthropogenic sources of CO_2 depending on the trajectory.

Zhang et al. (2006) demonstrated that the difference between the flux ratio and Keeling estimates of δ_R decreased as the Keeling plot integration time decreased. For instance, Keeling plots computed from 2-h time intervals or less showed much better agreement with the flux ratio estimate. This provides anecdotal evidence that part of the observed bias may be related to a change in background concentration and isotope ratio over longer time scales. During the non-growing season, when biological fluxes are small, $\delta^{13}C_a$ in the surface layer can vary diurnally by about 1.5‰ due simply to the effects of planetary boundary-layer (PBL) dynamics, including the transition from stable nighttime conditions to daytime growth and expansion of the PBL (Griffis et al. 2005a). Examination of the partial derivatives of Eq. 1c indicates that PBL dynamics (i.e. variations in $\delta^{13}C_a$ caused by PBL growth) influence the estimate of δ_R. For the above example, we would expect a sensitivity of approximately 0.55‰ for a 1 μmol mol^{-1} difference between the surface layer and so-called background air. Without examining changes in CO_2 mixing ratio and isotope ratio of the air mass along its back trajectory (a one-dimensional Lagrangian analysis) it is difficult to evaluate the full influence of air mass movement on the Keeling mixing model. It would seem reasonable to conclude from the above analyses that the difference between the flux ratio and Keeling methods at our particular field site is largely related to the extended footprint associated with a concentration measurement allowing contamination from upwind sources and perhaps to a lesser extent the influence of synoptic air mass change on the background CO_2 concentration and its isotopic composition.

The mismatch between the flux and concentration footprints may prove problematic for flux partitioning with Keeling-type approaches especially if fetch is limited with respect to the concentration footprint. The problem is more severe if a long integration time (i.e. a single night or day) is used to compute the Keeling intercept. Under these conditions, it appears that the Keeling parameters could be influenced by non-stationarity and changes in the background concentration and isotopic composition as the air mass originates from many kilometres upstream. The isoflux method (Flask/Keeling approach) has been used at a number of sites to estimate the

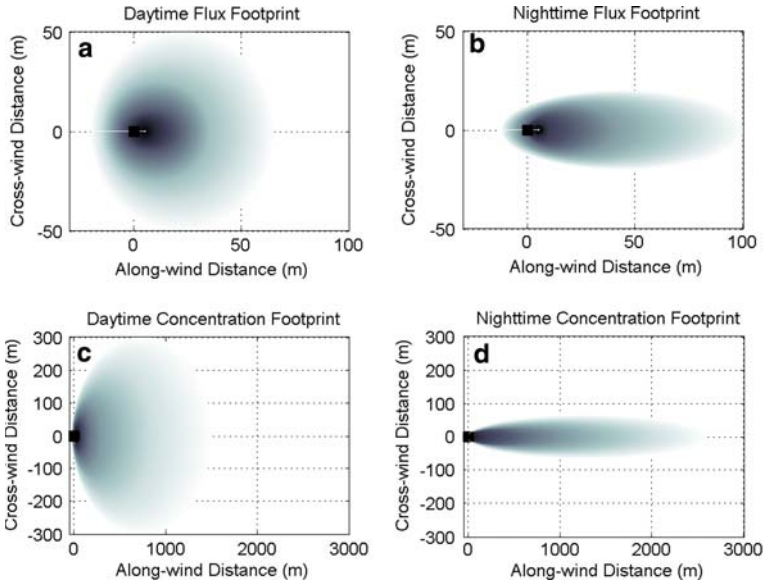

Fig. 11 A 90%-level source area for the daytime flux (**a**); nighttime flux (**b**); daytime concentration (**c**) and nighttime concentration (**d**). The grey shading represents the isopleths ranging up to 90% with darker shading indicating the area that the tower measurements are most sensitive to. All footprints were derived using the LPDM-B Lagrangian footprint model (Kljun et al. 2004)

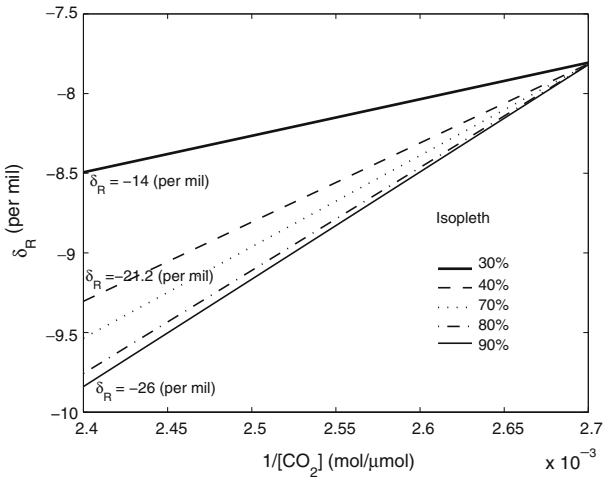

Fig. 12 Simple box model simulation of nighttime Keeling plots within a heterogeneous landscape. Each simulation represents a different relative source area according to the nighttime concentration footprint data presented in Fig. 11. The data shown correspond to the 30, 40, 50, 70, and 90% isopleths. The isotopic signature of the contributing source was weighted according to the footprint. For instance, in case 1 (30% isopleth) the source contribution is assumed to originate entirely from within the fetch of the field, yielding a Keeling intercept equal to the C_4 canopy (−14‰). The simulations demonstrate that the isotopic signature of ecosystem respiration (δ_R) is highly sensitive to the concentration footprint function (source area)

isotopic composition of F_N (Bowling et al. 2001; Lai et al. 2003; Ogée et al. 2003, 2004) and to isotopically partition the net exchange into its components. In this approach a Keeling-type transfer function ($\delta^{13}CO_2 = m[CO_2] + b$) is used to model rapid fluctuations in $\delta^{13}CO_2$. This linear function is developed from the mixing ratio and isotopic analysis of air captured in flasks over relatively long time intervals, typically ranging over the daytime or nighttime period. The transfer function is then used to estimate 10 Hz fluctuations in $\delta^{13}CO_2$ based on the input of real-time 10 Hz measurements of total CO_2 mixing ratio to estimate the approximate $^{13}CO_2$ flux using the eddy-covariance approach. While this innovative approach provides an attractive solution to estimating the $^{13}CO_2$ flux, the mismatch between the flux and Keeling mixing model footprints may limit its usefulness to only very special homogeneous situations. The sensitivity of isotopic flux partitioning to uncertainty in δ_N and δ_R can be very large and is dependent on the extent of isotopic disequilibrium. When isotopic disequilibrium is small ($< 3‰$) it can be shown that a 1‰ uncertainty in δ_R produces greater than 17% error in isotopic flux partitioning (Zhang et al. 2006). While we recognize that the Keeling method is a powerful tool, it is important to raise awareness of inherent scaling issues when combining these methods to quantify gross component fluxes and other key biophysical parameters. These issues deserve further attention as the micrometeorological and stable isotope communities continue to work toward combining these techniques to study carbon and water isotopic biosphere exchange processes.

4 Conclusions

The isotopic composition of ecosystem respiration (δ_R) was measured above a corn-soybean rotation ecosystem (fetch ≈ 200 m in all directions) over the course of three growing seasons within a heterogeneous agricultural landscape consisting of C_3 and C_4 ecosystems. Two approaches were used to quantify δ_R: the well-known mixing model (Keeling plot) and flux-gradient techniques. δ_R showed a strong and consistent pattern during each of the C_4 (corn) years, with values becoming more positive ($^{13}CO_2$ enriched) as the canopy developed and net ecosystem CO_2 exchange increased. Analysis of three years of high temporal resolution carbon isotopic data revealed a significant difference ($> 6‰$) between the mixing model and flux-gradient approaches for the C_4 canopy during peak growth. Understanding the causal factors between these two methodological approaches is important because representative values of δ_R at the ecosystem scale are needed to pursue isotopic flux partitioning and to improve the parameterization of land-surface and inversion type models.

A number of factors might account for the observed disparity between the mixing model and flux-gradient δ_R values. Excellent agreement between eddy-covariance and flux-gradient measurements of the total CO_2 flux prior to full canopy development suggests that differences in δ_R, about 3‰ at this time, were not related to a breakdown of Monin–Obukhov similarity theory or that the near-field effect biased the flux-gradient δ_R values. Therefore, measurements corresponding to the early growing period do not indicate that the concentration gradient was decoupled from the flux density canopy profile.

The dual footprint function could have important implications for determining the isotope signals and flux partitioning for taller vegetation, especially for oxygen isotopes in water vapour and carbon where the differences between vegetation and

soil can easily exceed 20‰. Our observations for C_4 corn canopies indicate that the carbon isotopic composition of in-canopy and above-canopy CO_2 fluxes was very similar, providing anecdotal evidence that the dual footprint does not significantly bias the isotopic flux ratio measurements at night when the Lagrangian time scale is relatively long and the near-field effect more important. Further, the isotopic composition of the in-canopy change in storage was similar to the isotopic composition of the above-canopy fluxes, providing additional evidence that the elevated source footprint under stable atmospheric conditions did not significantly weight the signal toward that of plant respiration.

Defining the footprint function of a mixing model (Keeling plot) is a difficult challenge, complicated by the fact that the model is typically based on observations collected over an extended time period (i.e. a nighttime period). It is no surprise that the footprint function of a concentration measurement is much greater than that for the flux. In the typical case presented here, the concentration footprint was nearly 20-fold greater than the flux footprint—extending out for a distance of about 2500 m. The mismatch between the Keeling plot footprint and the flux footprint functions has important implications for isotopic flux partitioning because the isotope signal may not necessarily represent the processes influencing the flux measurement due to land-surface heterogeneity. The situation is further complicated by the influence of air mass (back) trajectory because the slow change in background concentration and its isotopic composition is likely to have an impact on δ_R via the linear Keeling plot approach. Greater emphasis needs be placed on estimating isotope signals using flux-based approaches, especially for investigations at the ecosystem scale or sites that are located within heterogeneous terrain.

Acknowledgements We express our sincere thanks to Bill Breiter (USDA-ARS Biological Field Technician) for his assistance in the field and laboratory. The authors gratefully acknowledge the NOAA Air Resources Laboratory (ARL) for the provision of the HYSPLIT transport and dispersion model website (http://www.arl.noaa.gov/ready.html) used in this manuscript. Financial assistance for this project was provided by the Office of Science (BER), U.S. Department of Energy, Grant No. DE-FG02-03ER63684 (TJG & JMB). Finally, we recognize the helpful technical support of Steve Sargent at Campbell Scientific Inc.

References

Baker JM, Griffis TJ (2005) Examining strategies to improve the carbon balance of corn/soybean agriculture using eddy covariance and mass balance techniques. Agric For Meteorol 128:163–177

Bowling DR, Burns SP, Conway TJ, Monson RK, White JWC (2005) Extensive observations of CO_2 carbon isotope content in and above a high-elevation subalpine forest. Glob Biogeochem Cycles 19(3), Art. No. GB3023

Bowling DR, Sargent SD, Tanner BD, Ehleringer JR (2003) Tunable diode laser absorption spectroscopy for stable isotope studies of ecosystem–atmosphere CO_2 exchange. Agric For Meteorol 118:1–19

Bowling DR, Tans PP, Monson RK (2001) Partitioning net ecosystem carbon exchange with isotopic fluxes of CO_2. Global Change Biol 7:127–145

Ciais P, Friedlingstein P, Schimel DS, Tans PP (1999) A global calculation of the δ13C of soil respired carbon: Implications for the biospheric uptake of anthropogenic CO_2. Glob Biogeochem Cycles 13:519–530

Corrsin S (1974) Limitations of gradient transport models in random walks and turbulence. In: Frenkiel FN, Munn RE (eds) Turbulent diffusion in environmental pollution. Academic Press, New York, pp 25–60

Denmead OT, Bradley EF (1985) Flux-gradient relationships in a forest canopy. In: Hutchinson BA, Hicks BB (eds) The forest–atmosphere interaction. Reidel Publishing Co., Dordrecht, The Netherlands, pp 421–442

Flanagan LB, Kubien DS, Ehleringer JR (1999) Spatial and temporal variation in the carbon and oxygen stable isotope ratio of respired CO_2 in a boreal forest ecosystem. Tellus 51B:367–384

Flesch TK, Wilson JD, Yee E (1995) Backward-time Lagrangian stochastic dispersion models and their application to estimate gaseous emissions. J Appl Meteorol 34:1320–1332

Fung I, Field CB, Berry JA, Thompson MV, Randerson JT, Malmstrom CM, Vitousek PM, Collatz GJ, Sellers PJ, Randall DA, Denning AS, Badeck F, John J (1997) Carbon 13 exchanges between the atmosphere and biosphere. Glob Biogeochem Cycles 11:507–533

Griffis TJ, Baker JM, Sargent S, Tanner BD, Zhang J (2004) Measuring field-scale isotopic CO_2 fluxes using tunable diode laser absorption spectroscopy and micrometeorological techniques. Agric For Meteorol 124:15–29

Griffis TJ, Baker JM, Zhang J (2005a) Seasonal dynamics of isotopic CO_2 exchange in C_3/C_4 managed ecosystem. Agric For Meteorol 132:1–19

Griffis TJ, Lee X, Baker JM, Sargent S, King JY (2005b) Feasibility of quantifying ecosystem-atmosphere $C^{18}O^{16}O$ exchange using laser spectroscopy and the flux-gradient method. Agric For Meteorol 135:44–60

Kaimal JC, Finnigan JJ (1994) Atmospheric boundary layer flows: their structure and measurement. Oxford University Press, Inc., New York, 289 pp

Keeling CD (1958) The concentration and isotopic abundances of atmospheric carbon dioxide in rural areas. Geochim Cosmochim Acta 13:322–334

Kljun N, Kastner-Klein P, Fedorovich E, Rotach MW (2004) Evaluation of Lagrangian footprint model using data from wind tunnel convective boundary layer. Agric For Meteorol 127:189–201

Kljun N, Rotach MW, Schmid HP (2002) A three-dimensional backward lagrangian footprint model for a wide range of boundary-layer stratifications. Boundary-Layer Meteorol 103:205–226

Knohl A, Werner RA, Brand WA, Buchmann N (2005) Short-term variations in δ13C of ecosystem respiration reveals link between assimilation and respiration in a deciduous forest. Oecologia 142:70–82

Lai CT, Ehleringer JR, Tans P, Wofsy SC, Urbanski SP, Hollinger DY (2004) Estimating photosynthetic C-13 discrimination in terrestrial CO_2 exchange from canopy to regional scales. Glob Biogeochem Cycles 18(1), Art. No. GB1041.

Lai CT, Schauer AJ, Owensby, C, Ham JM, Ehleringer JR (2003) Isotopic air sampling in a tallgrass prairie to partition net ecosystem CO_2 exchange. J Geophys Res 108(D18), Art. No. 4566

Lee X (2003) Fetch and footprint of turbulent fluxes over vegetative stands with elevated sources. Boundary-Layer Meteorol 107:561–579

Lee XH (2004) A model for scalar advection inside canopies and application to footprint investigations. Agric For Meteorol 127:131–141

Lee X, Smith R, Williams J (2006) Water vapour $^{18}O/^{16}O$ isotope ratio in surface air in New England USA. Tellus 58B:293–304

Lloyd J, Kruijt B, Hollinger DY, Grace J, Francey RJ, Wong SC, Kelliher FM, Miranda AC, Farquhar GD, Gash JHC, Vygodskaya NN, Wright IR, Miranda HS, Schulze ED (1996) Vegetation effects on the isotopic composition of atmospheric CO_2 at local and regional scales: theoretical aspects and a comparison between rain forest in amazonia and a boreal forest in Siberia. Aust J Plant Physiol 23:371–399

Marschner FJ (1974) The original vegetation of Minnesota. U.S. Department of Agriculture, Forest Service. North Central Forest Experiment Station, St. Paul, MN. (Redraft of the original 1930 edition)

Meyers TP, Hall ME, Lindberg SE, Kim K (1996) Use of the modified bowen-ratio technique to measure fluxes of trace gases. Atmos Environ 30(19), 3321–3329

Ogée J, Peylin P, Ciais P, Bariac T, Brunet Y, Berbigier P, Roche C, Richard P, Bardoux G, Bonnefond JM (2003) Partitioning net ecosystem carbon exchange into net assimilation and respiration using (CO_2)-C-13 measurements: a cost-effective sampling strategy. Glob Biogeochem Cycles 17(2), Art. No. 1070

Ogée J, Peylin P, Cuntz M, Bariac T, Brunet Y, Berbigier P, Richard P, Ciais P (2004) Partitioning net ecosystem carbon exchange into net assimilation and respiration with canopy-scale isotopic measurements: an error propagation analysis with (CO_2)-C-13 and (COO)-O-18 data. Glob Biogeochem Cycles 18(2), Art. No. GB2019

Ometto JPHB, Flanagan LB, Martinelli LA, Moreira MZ, Higuchi N, Ehleringer JR (2002) Carbon isotope discrimination in forest and pasture ecosystems of the Amazon Basin, Brazil. Glob Biogeochem Cycles 16(4), Art. No. 1109

Pataki DE, Ehleringer JR, Flanagan LB, Yakir D, Bowling DR, Still CJ, Buchmann N, Kaplan JO, Berry JA (2003) The application and interpretation of Keeling plots in terrestrial carbon cycle research. Glob Biogeochem Cycles 17(1), Art. No. 1022

Randerson JT, Still CJ, Balle JJ, Fung IY, Doney SC, Tans PP, Conway TJ, White JWC, Vaughn B, Suits N, Denning AS (2002) Carbon isotope discrimination of arctic and boreal biomes inferred from remote atmospheric measurements and a biosphere–atmosphere model 9. Glob Biogeochem Cycles 16(3), Art. No. 1028

Raupach MR (1989) Stand overstorey processes. Philos Trans R Soc Lond B. 324:175–190

Rochette P, Flanagan LB, Gregorich EG (1999) Separating soil respiration into plant and soil components using analyses of the natural abundance of carbon-13. Soil Sci Soc Am J 63:1207–1213

Rotach MW (2001) Simulation of urban-scale dispersion using a Lagrangian stochastic dispersion model. Boundary-Layer Meteorol 99:379–410

Schmid HP (1994) Source areas for scalars and scalar fluxes. Boundary-Layer Meteorol 67:293–318

Schmid HP (2002) Footprint modeling for vegetation atmosphere exchange studies: a review and perspective. Agric For Meteorol 113:159–183

Seinfeld JH, Pandis SN (1998) Atmospheric chemistry and physics: from air pollution to climate change. John Wiley & Sons, Inc., New York, 1326 pp

Simpson IJ, Thurtell GW, Neumann HH, den Hartog G, Edwards GC (1998) The validity of similarity theory in the roughness sublayer above forests. Boundary-Layer Meteorol 87:69–99

Tans PP, Berry JA, Keeling RF (1993) Oceanic $^{13}C/^{12}C$ observation: a new window on ocean CO_2 uptake. Glob Biogeochem Cycles 7:353–368

Woodruff BL (1986) Sampling error in a single-instrument vertical gradient measurement in the atmospheric surface layer. MS thesis, Department of Atmospheric Science, Colorado State University, USA, 79 pp

Yakir D, Sternberg LDL (2000) The use of stable isotopes to study ecosystem gas exchange. Oecologia 123:297–311

Yakir D, Wang XF (1996) Fluxes of CO_2 and water fluxes between terrestrial vegetation and the atmosphere estimated from isotope measurements. Nature 380:515–517

Yepez EA, Williams DG, Scott RL, Lin GH (2003) Partitioning overstory and understory evapotranspiration in a semiarid savanna woodland from the isotopic composition of water vapor. Agric For Meteorol 119:53–68

Zhang J, Griffis TJ, Baker JM (2006) Using continuous stable isotope measurements to partition net ecosystem CO_2 exchange. Plant Cell Environ 29:483–496

Zobitz JM, Keener JP, Schnyder H, Bowling DR (2006) Sensitivity analysis and quantification of uncertainty for isotopic mixing relationships in carbon cycle research. Agric For Meteorol 136:56–75